CARBOXYMETHYL TAMARIND GUM-MEDIATED ENHANCEMENTS IN CITRIC ACID-CROSSLINKED CARBOXYMETHYLCELLULOSE HYDROGEL FILMS: OPTIMIZING MECHANICAL PROPERTIES, SWELLABILITY, DRUG LOADING CAPACITY AND SUSTAINED DRUG RELEASE

VISHWAJEET SAMPATRAO GHORPADE,[*] KAILAS KRISHNAT MALI,[**] NITIN HINDURAO SALUNKHE,[**] ROHIT DILIP GAIKWAD[**] and REMETH JACKY DIAS[***]

[*]*Department of Pharmaceutics, Krishna Institute of Pharmacy, Krishna Vishwa Vidyapeeth (Deemed to be University), Karad-415539, Maharashtra, India*
[**]*Department of Pharmaceutics, Adarsh College of Pharmacy, Near MIDC, Khambale (Bha.), Vita Tal-Khanapur 415311 Dist-Sangli, Maharashtra, India*
[***]*Department of Pharmacy, Government College of Pharmacy, Vidyanagar, Karad 415124, Tal-Satara, Maharashtra, India*
✉ *Corresponding author: K. K. Mali, malikailas@gmail.com*

Received August 15, 2025

Carboxymethyl tamarind gum (CMTG) and carboxymethyl cellulose (CMC) have emerged as promising biopolymers for hydrogel formation due to their excellent swelling properties and biocompatibility. Citric acid crosslinked CMC-CMTG hydrogel films have been developed for controlled delivery of moxifloxacin, a model drug, thereby addressing the limitations inherent in hydrogel films composed of individual polymers. The hydrogel films were synthesized through an esterification-crosslinking mechanism utilizing the solvent-casting technique. Characterization of the films was performed using ATR-FTIR, TGA, and solid-state ^{13}C NMR spectroscopy. Additionally, the films were evaluated for total carboxyl content, contact angle, tensile strength, swellability, drug loading, drug release, and hemocompatibility. The ATR-FTIR, TGA, and solid-state ^{13}C NMR analyses confirmed the formation of ester crosslinks between CMC and CMTG. The incorporation of CMTG enhanced the total carboxyl content, mechanical strength, and contact angle of the hydrogel films. However, the swellability and drug loading in the hydrogel films decreased with increasing concentrations of CMTG. All films demonstrated the capability to control the release of moxifloxacin for up to 24 h. The optimized batch (HFC) exhibited a tensile strength of 79.46 MPa, equilibrium swelling of 44.81±2.4 g/g in phosphate buffer (pH 7.4), drug loading of 464.70 mg/g, and released 87.46% of the drug at the end of 24 h. All hydrogel batches demonstrated controlled drug release characterized by non-Fickian (anomalous) diffusion kinetics. In conclusion, the results suggest that the citric acid-crosslinked CMC-CMTG hydrogel films exhibit superior mechanical strength, reduced matrix erosion, enhanced drug loading, and controlled drug release compared to hydrogels prepared using CMC and CMTG individually.

Keywords: carboxymethyl cellulose, carboxymethyl tamarind gum, hydrogel, citric acid, drug delivery

INTRODUCTION

Hydrogels are innovative materials that have greatly advanced the field of controlled drug delivery due to their unique properties, including biocompatibility, biodegradability, and high-water content, which facilitate drug encapsulation and sustained release. Hydrogels are three-dimensional networks of polymer chains characterized by their ability to swell and retain substantial amounts of water, attributed to hydrophilic functional groups such as –OH and –COOH, while remaining insoluble in water.[1,2] Both synthetic and natural polymers are employed in the preparation of hydrogels. However, synthetic polymer-based hydrogels may present toxicity concerns due to their low biodegradability. Consequently, natural polymer-based hydrogels are generally preferred. Natural polymers offer superior biocompatibility and biodegradability, rendering them environmentally friendly and more cost-effective than synthetic polymers.[3,4] Over the past two decades, there has

been an increasing emphasis on the development of natural hydrogels that exhibit extended longevity, high water absorption capacity, and enhanced mechanical strength.[1]

Traditional crosslinkers commonly employed in hydrogel synthesis include glutaraldehyde and epichlorohydrin.[5,6] Although these agents are effective in establishing crosslinked networks, they exhibit significant limitations, such as cytotoxicity, environmental hazards, and residual chemical impurities that may affect biocompatibility.[7] Citric acid is increasingly recognized as a non-toxic, environmentally friendly crosslinking agent for hydrogels derived from natural polymers, effectively addressing the limitations associated with traditional crosslinkers.[8] As a naturally occurring organic acid, citric acid can form ester linkages with the hydroxyl groups of polysaccharides, thereby establishing a crosslinked network without the toxicity typically associated with other chemical crosslinking agents.[9] Numerous studies have investigated the application of citric acid in crosslinking both natural and semi-synthetic polymers, such as starch, hydroxypropylmethyl cellulose (HPMC), carboxymethyl cellulose (CMC), hydroxyethyl cellulose (HEC), carboxymethyl tamarind gum (CMTG), and hydroxyethyl tamarind gum (HETG), demonstrating its versatility in producing hydrogels with tailored properties.[10–15]

CMC, derived from cellulose, is recognized for its excellent solubility in water, as well as its biodegradability and biocompatibility. It is employed in a range of industries, including food production, pharmaceuticals, and the development of biomaterials.[16] Upon crosslinking with citric acid, CMC forms hydrogel films that exhibit remarkable swellability, making them suitable for drug delivery systems. The swelling capacity of these hydrogel films is generally enhanced in neutral to basic environments, where the ionization of carboxyl groups facilitates increased water uptake due to electrostatic repulsion among the negatively charged groups, thereby expanding the network structure.[17] These hydrogels can regulate drug release rates through their swelling behavior and demonstrate non-Fickian release mechanisms.[18,19] Nonetheless, CMC hydrogel films face challenges such as low mechanical strength and rapid erosion rate post-equilibrium swelling, which may constrain their practical utility in drug delivery systems.[12,20] This limitation is potentially due to the formation of intramolecular rather than intermolecular crosslinks in CMC hydrogel films. Consequently, CMC is frequently combined with other polymers such as hydroxyethyl cellulose (HEC), polyvinyl alcohol (PVA), chitosan and tamarind gum (TG) for the fabrication of citric acid crosslinked hydrogel films.[18,21,22] It is observed that substituting a portion of CMC in the hydrogel films with these polymers enhances the mechanical strength and matrix integrity of CMC hydrogel films by increasing the crosslinking density, at the expense of reduced swellability, which may result in inferior drug loading compared to CMC hydrogel films alone.

CMTG is a modified polysaccharide derived from tamarind seed gum, which is known for its biocompatibility, hydrophilic properties, and versatility in drug delivery and tissue engineering applications.[23,24] Given the unique properties of CMTG, we prepared citric acid crosslinked CMTG hydrogel films for the delivery of the water-soluble drug, moxifloxacin.[25] Despite the presence of carboxyl groups, CMTG hydrogel films exhibited lower swellability than CMC hydrogel films, possibly due to a lesser degree of substitution in CMTG compared to CMC, yet demonstrated better resistance to matrix erosion and the ability to control drug release. We hypothesize that combining CMTG with CMC for the preparation of citric acid crosslinked hydrogel films may reduce matrix erosion by enhancing the mechanical strength of the hydrogel films without significantly affecting swellability, thereby controlling drug release more effectively than CMC hydrogel films.

In this study, citric acid-crosslinked CMC-CMTG hydrogel films were synthesized with the aim of enhancing mechanical strength, minimizing matrix erosion, and controlling the release of the model drug, moxifloxacin HCl (MFX). These hydrogel films are intended for biomedical applications, such as wound dressings and implantable drug delivery systems. The crosslinking between CMC and CMTG was confirmed through ATR-FTIR, TGA, and ^{13}C solid-state NMR analyses. The synthesized hydrogel films were subsequently evaluated for total carboxyl content, tensile strength, contact angle, swelling behavior, drug loading and release, and hemocompatibility.

EXPERIMENTAL

Materials

Carboxymethyl tamarind gum powder (average molecular weight: 9.14×10^5 g/mol, degree of

substitution: 0.28) was kindly gifted by Chhaya Industries, Barshi, Maharashtra (India). Carboxymethylcellulose (average molecular weight 250000, degree of substitution: 0.7, viscosity 575 cp) was gifted by Ashland, India. Citric acid (CA) was purchased from Loba Chemie, Mumbai, Maharashtra (India). Moxifloxacin hydrochloride (MXF) was generously provided as a gift sample by Chromo Laboratories, Sangareddy, Telangana, India. All other chemicals utilized in this study were of analytical grade and were used without further modification.

Methods

Synthesis of citric acid crosslinked CMC-CMTG hydrogel films

Hydrogel films were synthesized by reacting a mixture of CMC-CMTG with citric acid, following a previously reported method with slight modifications.[25] Briefly, a 2% w/v aqueous solution of the CMC-CMTG blend was prepared with continuous stirring at 1000 rpm using a mechanical stirrer (Remi, India) for 2 h. Subsequently, CA (0.4% w/v) was added, and the mixture was stirred for an additional 2 h. The solutions were then left undisturbed overnight to eliminate entrapped air bubbles. The aqueous solutions were poured into Petri dishes of uniform size (9 cm) and placed in a hot air oven (Ecogen, Equitron, India) at 50 °C for 24 h to remove water and form films of uniform size. The resulting films were cured at 145 °C for 5 min to achieve the desired crosslinking. The cured films were washed with an excess of distilled water to remove unreacted CA and polymer.[22] In brief, the films were immersed in 100 mL of distilled water and gently agitated on an orbital shaker for 10 min. This process was then repeated with fresh 100 mL portions of distilled water until the pH of the wash solution became neutral. Subsequently, the swollen films were washed with 100 mL of isopropyl alcohol (IPA) for 10 min, followed by 100 mL of acetone for an additional 10 min. The washed films were dried at 50 °C for 24 h and stored in a desiccator until use.[12] The weight loss and thickness of all batches were determined. The composition of the final batches of CMC-CMTG hydrogel films is detailed in Table 1. Additionally, CMC and CMTG hydrogel films were prepared for comparative analysis.

Table 1
Composition of CMC-CMTG hydrogel films

Batch	Ratio of CMC:CMTG	CA (% w/v)
HFA	9:1	0.4
HFB	8:2	0.4
HFC	7:3	0.4
HFD	6:4	0.4
HFE	5:5	0.4
CMC HF	1:0	0.4
CMTG HF	0:1	0.4

CMC: carboxymethyl cellulose; CMTG: carboxymethyl tamarind gum; CA: citric acid

Attenuated total reflectance Fourier transform infrared spectroscopy

Infrared spectra of CMC, CMTG, MFX, CA and hydrogel films were acquired using an ATR-FTIR Spectrophotometer (Alpha II, Bruker). Briefly, the samples for analysis were placed on the ATR, and spectra were recorded within the range of 600-4000 cm^{-1}, with an average of 25 scans and a resolution of 4 cm^{-1}.

Solid state ^{13}C NMR spectroscopy

The solid-state ^{13}C cross polarization-magic angle spinning (^{13}C CP-MAS) spectra of CMC, CMTG and CA crosslinked hydrogel films were acquired using a JEOL-ECX400 spectrometer operating at 400 MHz. The experimental parameters included a contact time of 3.5 ms, a relaxation delay of 5 s, a sweep width in kHz, and a spinning speed of 10 kHz. The chemical shifts were calibrated using an external hexamethylbenzene standard, with the methyl resonance set at 17.3 ppm.

Thermal analysis

Thermogravimetric analysis (TGA) and differential scanning calorimetry (DSC) were conducted on CMC, CMTG, CA and hydrogel films utilizing a TGA/DSC thermogravimetric analyzer (Mettler–Toledo, Switzerland). The samples were subjected to a temperature range from 30 °C to 500 °C at a heating rate of 10 °C per min, under a nitrogen atmosphere with a flow rate of 10 mL per minute.

Total carboxyl content of hydrogel films

The total carboxyl content (TCC) of hydrogel films was determined through acid-base titration, using phenolphthalein as an indicator.[26] Precisely, 100 mg of hydrogel films were weighed and dispersed in 20 mL of 0.1 N NaOH (free of CO_2). The resulting mixture was subjected to stirring using a magnetic stirrer (Remi, India) for a duration of two hours. Sodium hydroxide facilitates the breakdown of ester linkages and reacts with free carboxyl groups to form sodium carboxylate (citrate). This disrupts the integrity of the crosslinked

films, resulting in dispersion. The excess 0.1 N NaOH was subsequently titrated with 0.1 N HCl. The total carboxyl content of the hydrogel film was calculated using the following formula:

$$\text{Total Carboxyl Content} = \frac{(Vb - Va)\times N\times 100}{W} \quad (1)$$

where N is the normality of HCl (eq/L), Vb and Va are the volume of HCl in the absence and presence of sample, and W is the weight of sample (g).

Tensile strength of hydrogel films

The tensile strength of the hydrogel films was assessed utilizing a Texture Analyzer (CT-3/10,000, Brookfield, WI) equipped with a 10 kg load cell. A film sample measuring 2 × 1 cm was secured between the two clamps of the TA-DGA probe, with a hold time of 60 s. While the lower clamp remained stationary, the upper clamp was moved upward at a speed of 2.0 mm/s over a distance of 6 mm, with a trigger load set at 0.05 N. The force necessary to fracture the hydrogel film was recorded. Each test was conducted in triplicate. The tensile strength at the point of film rupture was calculated using the formula provided below:[27]

$$\text{Tensile strength (MPa)} = \frac{\text{Force at break (N)}}{\text{Initial cross-sectional area (mm}^2\text{)}} \quad (2)$$

Wetting behavior of hydrogel films

The wetting behavior of CA crosslinked CMC-CMTG hydrogel films was assessed using a manual water contact angle technique, as previously reported and slightly modified.[28] A 10 µL volume of distilled water was dispensed onto the hydrogel film surface using a microliter pipette. A digital camera captured the image of the droplet within 5 seconds. The image was analyzed using Image J software to measure the contact angle between the surface and the droplet. All measurements were conducted in triplicate.

Swelling study of hydrogel films

The swelling study was conducted utilizing a previously established method.[29] Precisely weighed hydrogel films (1 cm^2) were immersed in a phosphate buffer at pH 7.4 (10 mL). The swollen films were extracted at predetermined time intervals, extending up to 1440 minutes. Excess buffer on the films was blotted using tissue paper, and the swollen hydrogels were weighed with an analytical balance (Shimadzu, Japan). The swelling ratio was calculated using the following formula:

$$\text{Swelling ratio(g/g)} = \frac{(W_T - W_0)}{W_0} \quad (3)$$

where W_T is the weight of the swollen hydrogel film at time T, and W_0 is the weight of the dry hydrogel film before the study started. All measurement were done in triplicate.

Drug loading and release

The drug loading process involved immersing 500 mg of hydrogel film, cut into 1×1 cm pieces, in 20 mL of an aqueous solution of moxifloxacin hydrochloride (MFX) at a concentration of 10 mg/mL, allowing the film to swell until equilibrium was reached. The equilibrium swelling state of each hydrogel film in the MFX solution was determined by periodically measuring the weight of the swollen hydrogel until a constant weight was achieved, indicating equilibrium. The time to reach equilibrium was found to be dependent on the polymer composition and extent of crosslinking of the hydrogel batches. Subsequently, the films were dried in a hot air oven at 40 °C for 24 hours.

To quantify the drug loading in the hydrogel films, approximately 100 mg of the film was sectioned into small pieces and immersed in 50 mL of distilled water. This mixture was stirred using a magnetic stirrer (Remi, India) at 100 rpm for 24 hours, and the concentration of MFX was determined using a UV spectrophotometer (UV-1800, Shimadzu, Japan) at a wavelength of λmax 289 nm.[30,31] Distilled water was selected as the extraction medium because the preliminary studies indicated that solubility of MFX was nearly the same in distilled water and phosphate buffer (pH 7.4), ensuring complete drug extraction. Moreover, the drug loading was carried out using an aqueous MFX solution prepared in distilled water; therefore, the same medium was used for the determination of drug content to maintain consistency with the loading conditions.

The study of drug release from MFX-loaded hydrogel films was conducted in a phosphate buffer at pH 7.4 to simulate physiological conditions.[13,32] In summary, pre-weighed hydrogel films containing MXF were placed into vials with airtight caps, each containing 10 mL of phosphate buffer at pH 7.4. These vials were maintained at a constant temperature of 37 °C. At predetermined intervals, samples were withdrawn from the vials and replaced with fresh dilution medium to maintain sink conditions. The samples were then filtered, diluted, and analyzed for MXF content using a UV spectrophotometer (UV-1800, Shimadzu, Japan) at 289 nm. The study was performed in triplicate. The dissolution kinetics of the release data were fitted to zero-order, first-order, Higuchi, and Korsmeyer-Peppas models.[33]

Hemocompatibility study of hydrogels

The hemolysis assay was conducted following the method previously described.[13,18] A piece of hydrogel film with an area of 2 cm^2 was allowed to swell in phosphate-buffered saline (PBS) maintained at 37 °C for 1 hour. Subsequently, the PBS was removed, and 0.5 mL of human CPD (citrate phosphate dextrose) blood was added to the film. After 20 minutes, 4.0 mL of 0.9% sodium chloride solution (NaCl) was added to each sample to halt hemolysis, and the samples were incubated for an additional hour at 37 °C. The incubated samples were then centrifuged at 4000 rpm for 10 minutes, and the supernatant was subjected to spectrophotometric analysis (UV-1800 Shimadzu, Japan) at 545 nm. The positive control consisted of 0.5 mL of human CPD blood and 4 mL of double-distilled

water, while the negative control comprised 0.5 mL of 0.9% NaCl saline and 4 mL of double-distilled water. The following formula was employed to determine the percentage of hemolysis:

$$\text{Hemolysis}(\%) = \left(\frac{A_{\text{test sample}} - A_{-\text{ve control}}}{A_{+\text{ve control}} - A_{-\text{ve control}}}\right) \times 100 \quad (4)$$

where A is absorbance.

Statistical analysis

The numerical data were subjected to statistical analysis using one-way ANOVA, followed by Tukey's multiple comparison tests. A p-value of less than 0.05 was considered statistically significant.

RESULTS AND DISCUSSION

Synthesis of citric acid crosslinked CMC-CMTG hydrogel films

CMC is a cellulose derivative with some hydroxyl groups on the β-D-glucopyranose units of the cellulose backbone substituted with carboxymethyl groups. Due to this modification, CMC exhibits enhanced water solubility and viscosity. CMC used in this study had a DS of 0.7, indicating 70% of the hydroxyl groups were substituted with carboxymethyl groups.[34] It has been reported that in the presence of polycarboxylic acid crosslinkers, CMC forms intramolecular crosslinks rather than interpolymer crosslinks because its carboxyl and hydroxyl groups react preferentially within the CMC chain due to spatial proximity and steric factors.[35–37] On the other hand, CMTG is a galactoxyloglucan composed of a β-1,4-glucose backbone with xylose and galactose side branches.[38] Its branched structure introduces steric hindrance and additional sites for intermolecular interactions and crosslinking when combined with other polymers. Compared with CMC, the branched structure of tamarind gum leads to a lower degree of substitution (DS = 0.28), indicating fewer carboxymethyl groups per sugar unit. This leads to reduced swellability in CMTG compared to CMC.

The formation of CA crosslinked CMC-CMTG hydrogel films was achieved through an esterification reaction. Upon heating CA with CMC-CMTG at elevated temperatures, CA is converted into its anhydride form. This anhydride subsequently esterifies the hydroxyl (–OH) groups present in both CMC and CMTG, leading to the establishment of ester crosslinks between the polymer chains. Figure 1 illustrates the synthesized CMC-CMTG hydrogel film and the proposed esterification reaction responsible for its formation.

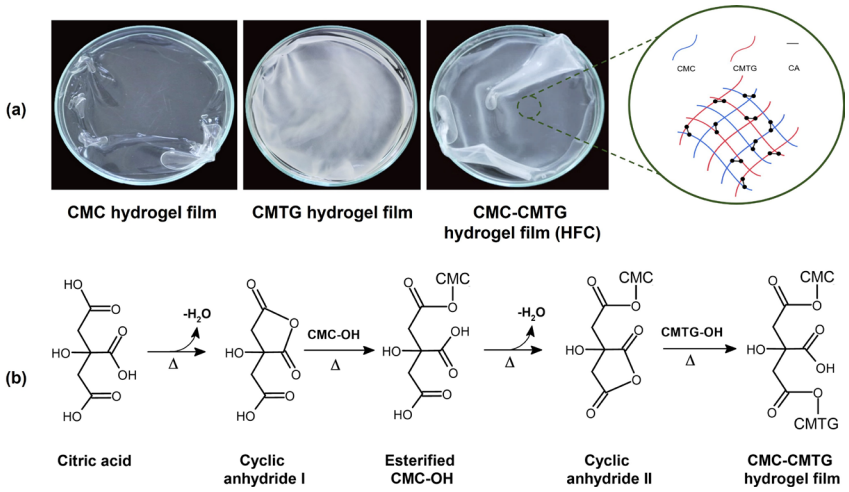

Figure 1: Synthesized CMC, CMTG, CMC-CMTG hydrogel films (a) and proposed esterification reaction for the formation of CMC-CMTG hydrogel film

The preformulation study was conducted to ascertain the optimal concentrations of CMC, CMTG, and citric acid, as well as to optimize curing time and temperature to establish suitable experimental conditions. Initially, the focus was on optimizing polymer concentration to achieve optimal hydrogel film formation. The polymer concentration was increased from 1% to 4%, while maintaining a constant CA concentration, which resulted in a decrease in crosslinking density. At the lower polymer concentration (1% w/v), the film appeared rigid and did not swell in distilled water, whereas at higher concentrations (>2% w/v), the film became brittle, fragile, and formed a gel upon exposure to distilled water due to intra-crosslinking of polymeric chains. Based on these

observations, a 2%w/v polymer concentration was deemed sufficient to produce inter-crosslinks between polymeric chains. Consequently, it was decided to use a 2% w/v polymer concentration for subsequent batches to achieve balanced characteristics of hydrogel films.

During the preformulation batches, the concentration of CA was adjusted within the range of 0.2 to 0.6% w/v. It was observed that when the CA concentration exceeded 0.4% w/v, the crosslinking density increased, resulting in rigid films with reduced water retention capacity. This outcome was attributed to enhanced inter-polymer crosslinking, possibly caused by decreased polymer chain mobility and reduced free space within the crosslinked polymer networks. Conversely, at lower concentrations of CA (< 0.4% w/v), hydrogel film formation was hindered due to inadequate crosslinking, potentially leading to compromised film integrity. Therefore, a CA concentration of 0.4% w/v was selected to achieve optimal water retention capacity and film integrity.

To optimize the curing temperature and duration for the hydrogel films, variations were implemented ranging from 130 °C to 150 °C, with curing times spanning from 5 to 15 minutes. At lower temperatures and shorter durations, the crosslinking with citric acid was inadequate, resulting in gel formation rather than the intended crosslinked structure. Conversely, at elevated temperatures (150 °C) and extended curing times (15 min), the films became excessively rigid and lost their capacity for water retention.

Following experimentation, it was established that a curing temperature of 145 °C and a curing duration of 5 minutes were adequate to produce hydrogel films exhibiting excellent structural integrity and high water retention capacity. Consequently, these parameters were adopted for subsequent batches. The final batches of CMC-CMTG hydrogel films were prepared utilizing a 2% polymer blend and 0.4% CA, with a curing temperature of 145 °C and a curing time of 5 min.

Weight loss and thickness of hydrogel films

The weight loss of CA crosslinked hydrogel films, following sequential washing with distilled water, isopropyl alcohol, and acetone, is detailed in Table 2. The weight loss of these hydrogel films ranged from 21.25% to 29.56%. The CA crosslinked CMC hydrogel film exhibited a weight loss of 29.56%. We assume that it is likely due to the formation of a loosely crosslinked network structure, which permits the dissolution of unreacted polymer and CA. In contrast, the CA crosslinked CMTG hydrogel film demonstrated a weight loss of 21.25%. The comparatively lower weight loss observed in the CMTG film is attributed to the probable formation of a dense network structure, which restricts the dissolution of unreacted polymer. Furthermore, in the case of CA crosslinked CMC-CMTG hydrogel films, an increase in CMTG concentration resulted in a decrease in weight loss from HFA to HFE. The reduction is likely due to an increase in the formation of ester crosslinks between CMC and CMTG chains, which may create a dense network within the polymer matrix. This network structure reduces the removal of unreacted macromolecules from the film.[18]

The thickness of CA crosslinked hydrogel films of CMC-CMTG was determined using a micrometer screw gauge, as shown in Table 2. The CMC hydrogel film alone exhibited a thickness of 660 µm, while the CMTG hydrogel film alone showed a thickness of 587 µm. Hydrogel films from HFA to HFE displayed thicknesses ranging from 591 µm to 632 µm. An increase in CMTG concentration corresponded with an increase in the thickness of the hydrogel films, possibly due to an increase in the crosslinking density of the films. Such an increase in crosslinking can result in a denser network, which may create more extensive three-dimensional structures, leading to thicker films. Higher crosslinking density can increase film thickness by creating a more robust and extended polymer network.[39,40]

Total carboxyl content of hydrogel films

The total carboxyl content (TCC) of hydrogel films encompasses both the free carboxyl groups inherent in the polymer and those generated due to the rupture of ester crosslinks upon exposure to NaOH. The presence of both free carboxylic acids and ester carboxylate groups in the ester crosslink of hydrogel films is a significant aspect of their composition. When 0.1N NaOH is added to the hydrogel films, it initiates the breakdown of the ester crosslinks. NaOH reacts with both the preexisting and newly formed free carboxyl groups, resulting in the formation of sodium carboxylate. By measuring the amount of NaOH that reacts with the carboxyl groups in the hydrogel films, we determined the total carboxyl content of the hydrogel. This method allows for the quantification of all carboxyl groups present in the hydrogel, including those involved in ester crosslinks and any free carboxyl groups that may

be present. TCC serves as an indirect indicator of the crosslinking density of the hydrogel films and provides insight into their swellability in given medium.[13]

TCC of the hydrogel films was determined to range from 371.67 mEq/100g to 452.33 mEq/100g (see Table 2). An increase in the concentration of CMTG within the hydrogel film resulted in a statistically significant enhancement in TCC ($p>0.05$) from batch HFA to HFD. This phenomenon can be attributed to an increase in the formation of ester crosslinks between CMC and CMTG as the amount of CMTG continues increasing. This indicates that the incorporation of CMTG facilitates the formation of interpolymer crosslinks, which may result in an increase in the crosslinking density of the hydrogel films. The TCC values of hydrogel films composed exclusively of CMC (CMC HF) and CMTG (CMTG HF) were found to be consistent with the values reported in our previous studies.[12,25] The higher TCC observed in CMTG hydrogel films, despite their lower degree of substitution compared to CMC, may be due to extensive ester crosslinking during CA treatment. The TCC method measures both free carboxyl groups and those released from ester bonds during NaOH titration; hence, a higher crosslink density in CMTG leads to a greater apparent TCC. Although CMC has high DS, the extent of interpolymer crosslinking in CMC hydrogel films may be lower, resulting in reduced TCC.

Table 2
Weight loss, thickness, TCC, peak intensity ratio and tensile strength of hydrogel films

Batch	Weight loss (%)	Thickness (μm)	TCC (mEq/100g)	$I_{\sim 1725/\sim 2916}$	Tensile strength (MPa)	Contact angle (θ°)
HFA	26.72±0.69	591.67±2.89	371.67±4.51	0.561	63.38±1.71	65.54±2.11
HFB	25.83±0.43	612.00±3.04	400.83±4.86	0.612	65.71±2.18	67.89±1.57
HFC	25.69±0.38	613.67±3.18	427.33±4.73	0.688	79.46±1.76	71.87±1.09
HFD	25.56±0.41	621.83±2.75	436.67±5.77	0.718	87.13±2.46	73.61±2.05
HFE	24.00±0.42	632.00±3.04	442.33±5.13	0.818	93.32±1.62	74.41±1.16
CMC HF	29.56±0.46	660.31±2.27	246.12±4.93	0.487	61.91±1.89	62.75±2.37
CMTG HF	21.25±0.55	587.00±2.60	558.33±5.86	0.301	85.37±1.58	71.98±2.64

TCC: total carboxyl content; $I_{\sim 1725/\sim 2916}$: peak intensity ratio

ATR-FTIR study of hydrogel films

The ATR-FTIR spectra of CMC, CMTG, and CA crosslinked films are illustrated in Figure 2. The ATR-FTIR spectrum of CMC exhibits distinct characteristic bands. A broad peak at 3100 cm^{-1} signifies -OH stretching vibrations, accompanied by medium peaks at 2831 cm^{-1} and 2879 cm^{-1}, indicating asymmetric -CH stretching. Furthermore, the presence of a peak at 1744 cm^{-1} indicates C=O stretching of the ester group. The peaks at 1587 cm^{-1} and 1410 cm^{-1} confirm the presence of carboxyl groups in CMC, while the peak at 1023 cm^{-1} denotes C-O-C stretching of the glycosidic linkage of CMC (Fig. 2a). The CMTG spectrum (Fig. 2b) displays similar functional group bands, but with distinct shifts and intensities that reflect its unique polysaccharide structure.

The ATR-FTIR spectrum of the CA-crosslinked CMC film (Fig. 2a) exhibits a minor absorption peak at 1723 cm^{-1} suggesting the presence of ester carbonyl groups.[41,42] Similarly, the ATR-FTIR spectrum of the CA-crosslinked CMTG hydrogel film (Fig. 2b) shows a small peak at 1734 cm^{-1}, which is indicative of the carbonyl stretching of ester groups.[30] The presence of these minor peaks at 1723 cm^{-1} (CMC) and 1734 cm^{-1} (CMTG) confirms the formation of ester crosslinks in both the CMC and CMTG hydrogel films. The ATR-FTIR spectrum of the CA-crosslinked CMC-CMTG hydrogel films is shown in Figure 3. Notably, the intensity of the 1725 cm^{-1} peak increases with rising CMTG content (from HFA to HFE), which can be attributed to the formation of CMC–CMTG crosslinks rather than intramolecular crosslinks, which may increase the crosslink density.[13,41]

This observation is further supported by the increasing ratio of the intensity of the ~1725 cm^{-1} peak to that of the peak at ~2916 cm^{-1} (-CH stretching) with an increase in CMTG concentrations, as presented in Table 2.[43] The findings align with the results of TCC, indicating that an increase in CMTG content may boost the degree of crosslinking in hydrogel films.

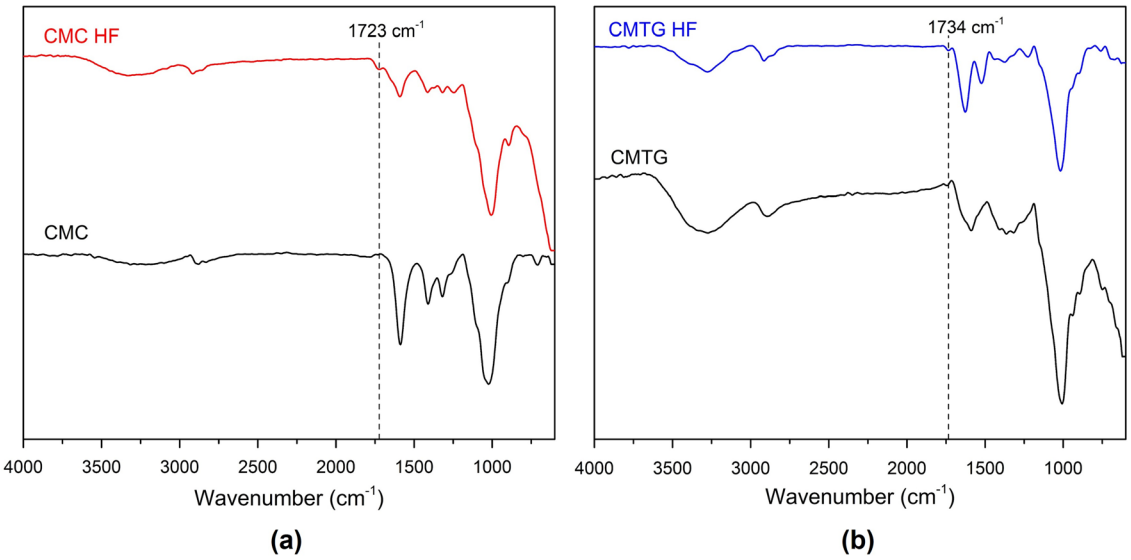

Figure 2: ATR-FTIR spectra of CMC and CMC HF (a), and CMTG and CMTG HF (b)

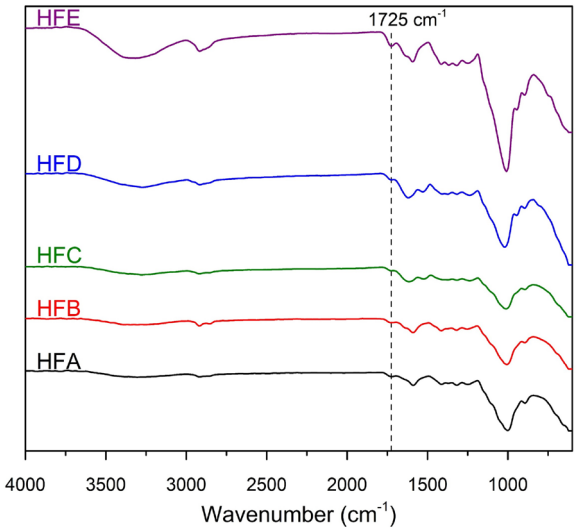

Figure 3: ATR-FTIR spectra of CA crosslinked CMC-CMTG hydrogel films

Thermogravimetric analysis of hydrogel films

Figure 4a shows the TGA curves for CMC, CMTG, CA, and hydrogel films. CMTG decomposed in three stages: 30–130 °C (10.36% mass loss, moisture removal), 130–260 °C (4.21% loss), and 260–330 °C (38.03% loss, backbone degradation), resulting in 69.59% total loss at 500 °C. CMC displayed similar stages: 30–110 °C (9.04%), 110–260 °C (3.76%), and 260–320 °C (39.33%), with 62.81% total loss at 500 °C, confirming greater thermal stability than CMTG. The CMTG hydrogel film lost 5.63% (30–150 °C), 14.68% (150–240 °C), and 34.87% (240–340 °C), with total weight loss of 64.45% at 500 °C, indicating improved stability over pure CMTG. The CMC film lost 7.70% (30–170 °C), 12.21% (170–290 °C), and 39.34% (290–350 °C), with 73.26% total loss at 500 °C. CMC–CMTG hydrogels (Fig. 4a) also exhibited three degradation stages, with total mass losses from 68.56% (HFA) to 64.68% (HFE) at 500 °C. This reduction in mass loss can be attributed to an increased residual char formation and resistance to the volatilization probably due to enhanced crosslinking with a decrease in the CMC:CMTG ratio in the hydrogel films. Besides, CMC-CMTG hydrogel films may be denser, stiffer, more robust due to CMTG, which has a branched structure, unlike CMC, which is a linear, flexible polymer, which could lead to a decrease in the mass loss.

Figure 4b shows the DTG thermograms of CMC, CMTG, and citric acid–crosslinked CMC–CMTG hydrogel films (HFA–HFE), and Table 3 lists the onset temperature (T_o), maximum degradation temperature (T_m) and endset temperature (T_e) for these samples. For the CMC hydrogel film, T_o, T_m, and T_e were higher than for the CMTG film, demonstrating that CMC exhibited higher thermal stability than CMTG.[44] As the CMTG content increased and CMC decreased from HFA to HFE, T_o was found to be increased, indicating enhanced network rigidity due to enhanced crosslinking. It was observed that T_m initially rose from 279.79 °C (HFA) to 299.24 °C (HFB), reflecting optimal crosslink density, but then declined to 250.23 °C (HFD and HFE), suggesting that excessive CMTG introduces steric hindrance and residual unreacted branches that reduce thermal resistance in highly crosslinked hydrogels.[45] On the other hand, T_e reduced from HFA to HFE, which can be ascribed to the tighter, char-forming degradation of the denser network.[46]

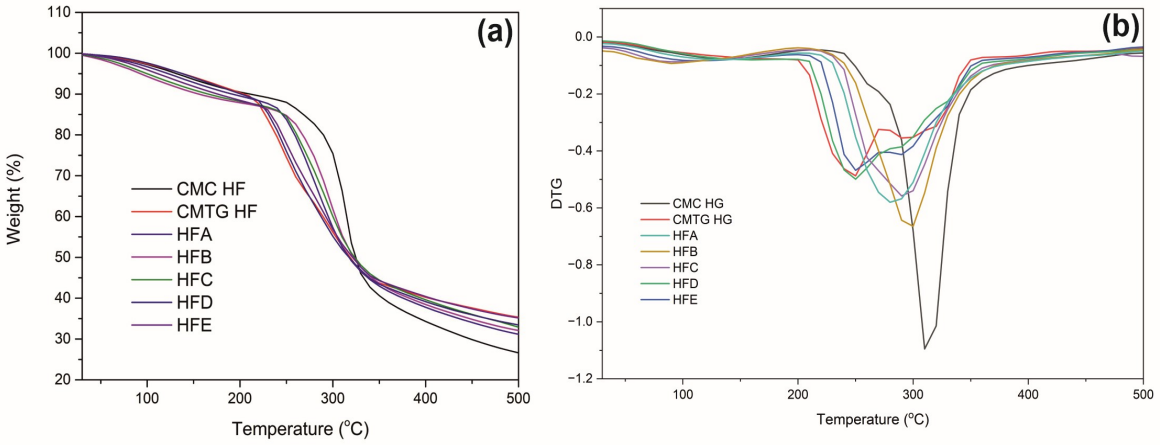

Figure 4: Thermal analysis: (a) TGA and (b) DTG thermograms of CMC-CMTG hydrogel films (HFA–HFE)

Table 3
Thermal degradation parameters and mass loss (%) of CMC, CMTG and CMC–CMTG hydrogel films (HFA–HFE)

Batch	T_o (°C)	T_m (°C)	T_e (°C)	Mass loss (%)			Residue* (%)
				Stage I	Stage II	Stage III	
HFA	204.80	279.79	390.11	8.73	13.27	32.37	33.59
HFB	205.73	299.24	381.70	6.58	17.27	34.37	31.55
HFC	209.46	290.06	379.83	9.28	9.78	37.32	25.87
HFD	209.46	250.23	371.59	6.06	6.88	38.93	30.09
HFE	210.41	250.23	360.39	4.52	15.65	30.42	29.05
CMC HF	239.96	309.51	391.82	7.7	12.21	39.35	21.16
CMTG HF	199.35	250.23	361.32	5.63	14.68	34.87	33.64

T_o – onset temperature; T_m – maximum degradation temperature; T_e – endset temperature; *Residue at 500 °C

Solid state ^{13}C NMR

Figure 5 presents the solid-state ^{13}C NMR spectra of CMC, CMTG and CMC-CMTG hydrogel films (HFC), alongside the structure of their constituent monosaccharide units – glucose in both CMC and CMTG, and galactose and xylose in CMTG. Solid-state ^{13}C NMR provides detailed information on the chemical environment of each carbon atom and functional group within these polymer matrices.[47]

In the spectrum of pure CMC, four main resonance regions are evident: C6 at 62.57 ppm; a cluster of C2, C3, C5, and C7 between 66–80 ppm; C4 at 80–90 ppm; and the anomeric C1 from 94–110 ppm. A distinct peak at 178.02 ppm corresponds to the carboxyl carbon of the carboxylate moiety.[48] In the case of the CMC hydrogel film (CMC HF), the C1 and C6 signals shifted slightly downfield, while C2–C5 moved upfield, reflecting the altered electronic environment induced by CA-mediated

crosslinking. Notably, the carboxylate carbon peak broadened and shifted to 177.76 ppm, consistent with the formation of ester linkages and residual free –COOH groups.[47,49]

Pure CMTG exhibited analogous resonance regions: C6 at 57–66 ppm; the hydroxyl-bearing carbons (C2,2*,2′; C3,3*,3′; C5,5*,5′; C7) between 66–80 ppm; C4,4*,4′ at 80–90 ppm; and the anomeric carbons (C1,1*,1′) from 92–112 ppm. Its carboxylate carbon peak appeared at 172.5 ppm. In the CMTG hydrogel film (CMTG HF), C1 shifted downfield and C2–C5 shifted upfield, mirroring the behavior seen in CMC HF due to crosslink formation. The carbonyl resonance broadened and moved to 171.95 ppm, further indicating esterification and presence of unreacted carboxyl groups.[14,25]

The composite hydrogel film (HFC) spectrum combines features of both polymers: C6 at 56–66 ppm; C2,2*,2′; C3,3*,3′; C5,5*,5′; C7 between 66–80 ppm; C4,4*,4′ at 80–91 ppm; and C1,1*,1′ from 94–109 ppm. A broad resonance centered at 177.68 ppm signifies overlapping carboxylate carbon signals from ester crosslinks and free –COOH groups. Moreover, this peak broadened from 165–185 ppm, which indicates that CMC–CMC, CMC–CMTG, and CMTG–CMTG crosslinking all occur together in the CMC-CMTG hydrogel films.[14,41,47] The peak at 177.68 ppm was further validated by employing the Voigt function within the peak fitting module of OriginPro 9.0.0 software (OriginLab Corporation, USA).

The Voigt-profile deconvolution of the 165–185 ppm region of solid state ^{13}C NMR spectrum of CMC–CMTG composite hydrogel film exhibited three overlapping carbonyl resonances (see Fig. 6). The highest-frequency component at 179.23 ppm is attributed to unreacted carboxylate groups and residual free –COOH moieties, indicating segments of CMC and CMTG chains that did not undergo esterification. The intermediate peak at 176.84 ppm is primarily associated with ester linkages formed by intramolecular crosslinking within CMC chains (CMC–CMC). Lastly, the lower-frequency signal at 174.79 ppm originates from intermolecular ester bonds between CMC–CMTG, as well as potential CMTG–CMTG crosslinks.

The results from ATR-FTIR, thermal analysis, and solid-state ^{13}C NMR indicated that increasing the amount of CMTG in the CMC hydrogel films enhanced the degree of crosslinking in the CMC-CMTG hydrogel films.

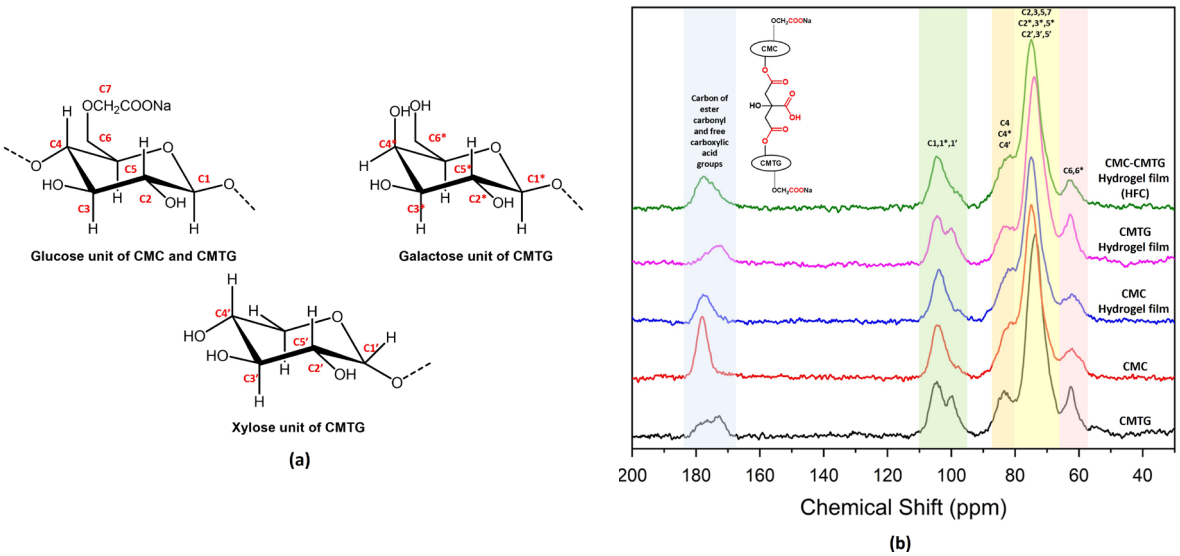

Figure 5: Chemical structures of glucose (CMC and CMTG), galactose (CMTG) and xylose (CMTG) units (a), and solid-state 13C NMR spectra of CMC, CMTG, CMC hydrogel film, CMTG hydrogel film, and a CMC-CMTG blended hydrogel film (b)

Tensile strength of hydrogel films

The tensile strength results highlight the influence of polymer composition and crosslinking density on the mechanical properties of the hydrogel films. The pure CMC hydrogel film (CMC HF) exhibited the lowest tensile strength of 61.91 Mpa, a result attributed to the relatively flexible cellulose backbone and the limited crosslinking sites available for CA esterification.[49] In contrast, CMTG HF showed superior mechanical strength (85.37 MPa) due to the inherent rigidity of the galactoxyloglucan

structure, where the galactose and xylose side chains provide additional steric hindrance and intermolecular interactions that enhance film integrity.[25]

The gradual enhancement in tensile strength seen in the CMC–CMTG composite films (HFA–HFE) as the CMTG content rises highlights the combined effect of mixing these polysaccharides (see Table 2). As confirmed by our solid-state ^{13}C NMR deconvolution analysis, the composite films exhibit a complex network of CMC–CMC, CMC–CMTG, and CMTG–CMTG crosslinks mediated by CA. The peak tensile strength achieved by HFE indicates an optimal balance between crosslinking density and polymer chain mobility, where sufficient CMTG content provides enhanced structural rigidity, while maintaining adequate chain flexibility for stress distribution. This mechanical reinforcement aligns with the thermal stability improvements observed in TGA analysis and the extensive ester bond formation evidenced by ATR-FTIR and solid-state ^{13}C NMR spectroscopy, collectively demonstrating that CMTG incorporation creates a more robust three-dimensional network structure.

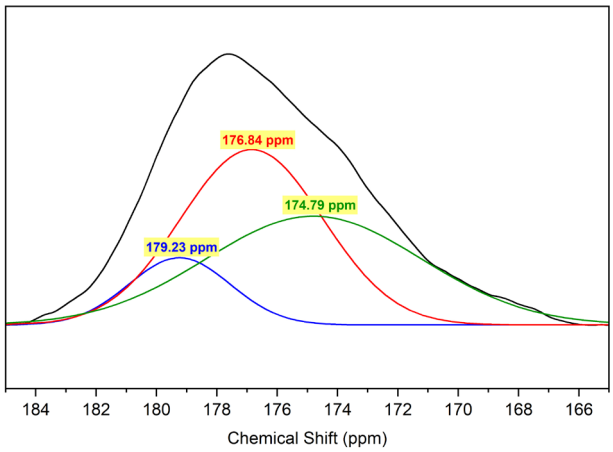

Figure 6: Voigt deconvolution of the 165–185 ppm carbonyl region of CMC-CMTG composite hydrogel film

Wettability of hydrogel films

Wettability behavior describes how a liquid interacts with a solid surface. In hydrogel films, wettability plays an important role for assessing their effectiveness and suitability in drug delivery systems and biomedical devices. Studying wettability offers insights into the interaction of biological molecules with biomaterials, where a lower contact angle indicates higher hydrophilicity, and a higher contact angle suggests lower hydrophilicity and a more hydrophobic surface. Both CMC and CMTG are naturally hydrophilic due to their hydroxyl groups. The contact angle measurement results are shown in Table 2. All hydrogel films demonstrated hydrophilic properties, with measured angles ranging from 62.75° to 74.41°, confirming adequate wetting of the hydrogel with water. CMC (CMC HF) exhibited significantly ($p>0.05$) higher hydrophilicity (62.75±2.37°) compared to CMTG (CMTG HF) (71.98±2.64°). This is attributed to the abundant free –OH and –COOH groups in CMC HF. In CMTG HF, the presence of a more rigid, less polar galactoxyloglucan backbone reduces surface energy, thereby decreasing hydrophilicity. For HFA-HFE, as the concentration of CMTG increased, the contact angle also increased significantly ($p>0.05$), indicating reduced hydrophilicity. This suggests that a decrease in the CMC:CMTG ratio enhances ester crosslinking, which not only stiffens the network, but also lowers surface polarity, resulting in progressively more hydrophobic surfaces.[28,42]

Swelling study of hydrogel films

A hydrogel is a three-dimensional hydrophilic network of polymers that, upon contact with water, swells and retains a significant amount of fluid. The extent of swelling of the crosslinked matrix is influenced by the extent of crosslinking within the hydrogel films and the physicochemical characteristics of the polymers used. Swelling is a crucial parameter for various applications such as drug loading, drug release, and *in vivo* absorption of exudates.[13,50]

In order to evaluate the potential of the prepared hydrogel films as biomaterials for drug delivery, swelling studies were conducted in a phosphate buffer at pH 7.4. The equilibrium swelling ratio (ESR) results for the hydrogel films are presented in Table 4, while Figure 7a illustrates the swelling behavior of CA crosslinked hydrogel films. Consistent with our previous studies, CMC hydrogel films (CMC HF) demonstrated greater swellability (higher ESR) compared to CMTG hydrogel films (CMTG HF). This difference can be attributed to the higher presence of free COOH and -COONa groups in CMC HF, which ionize at pH 7.4, leading to electrostatic repulsion between the polymer chains of the hydrogel films. Consequently, CMC HFs can accommodate more water than CMTG HFs. Notably, batches HFA, HFB, and HFC exhibited even higher swellability than both CMC HF and CMTG HF. This could be due to two factors. Firstly, CMC contains highly hydrophilic COONa groups that dissociate in aqueous media, creating electrostatic repulsion between polymer chains and enhancing water uptake. Although CMTG contains fewer COONa groups than CMC, it provides additional hydroxyl groups and moderate hydrophilicity. When CMC and CMTG are combined to form CMC-CMTG hydrogel films, an optimal balance may be achieved, where CMC provides the primary ionic contribution for swelling, while CMTG contributes to structural stability and additional hydrophilic sites without excessive self-entanglement, resulting in higher swellability than CMC HF and CMTG HF.[51] Secondly, the addition of CMTG to CMC may promote intermolecular crosslinking between CMC and CMTG rather than intramolecular crosslinks. This could create a more organized network structure in the hydrogel matrix than in CMC HF and CMTG HF, which can help retain more water in the matrix in the case of HFA-HFC.[52] As the CMC:CMTG ratio decreased, the swellability of the hydrogel films reduced, and more time was required to achieve ESR. This could be due to an increase in the extent of interpolymer crosslinks, which restricts water penetration into the hydrogel matrix and reduces water retention. Batch HFA exhibited the highest equilibrium swelling ratio of 55.14 g/g, whereas batch HFE displayed a lower equilibrium swelling ratio of 14.04 g/g. It was observed that CMC-CMTG hydrogel films showed a slower rate of erosion post-equilibrium up to 24 h compared to CMC HF and CMTG HF (see Fig. 7b). A decrease in the CMC:CMTG ratio led to a decrease in the rate of erosion in the CMC-CMTG hydrogel films up to 24 h, with HFE exhibiting good resistance to erosion during this period. This confirmed that combining CMTG with CMC improved the matrix integrity of the hydrogel films up to 24 h.

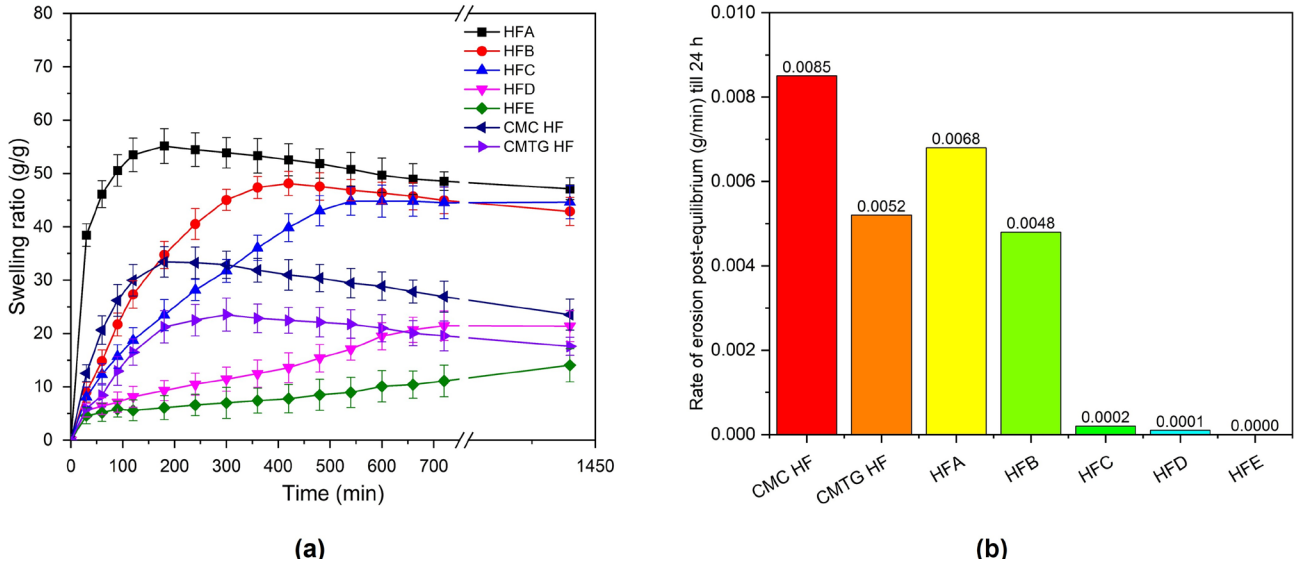

Figure 7: Swelling ratio of hydrogel films in phosphate buffer pH 7.4 (a), and rate of erosion of hydrogel films post-equilibrium till 24 h

Table 4
Equilibrium swelling ratio (ESR), drug loading and percent drug released at the end of 6h (Q_{6h})

Batch	ESR (g/g of hydrogel film)	Drug loading (mg/g)	Q_{6h} (%)
HFA	55.14 ± 3.27	505.94	69.11
HFB	48.12 ± 2.25	485.84	70.26
HFC	44.81 ± 2.82	464.70	78.51
HFD	21.44 ± 2.77	320.71	85.78
HFE	14.04 ± 3.12	237.23	91.10
CMC HF	33.42 ± 2.82	496.53	80.25
CMTG HF	23.54 ± 2.09	113.32	82.26

Drug loading

The drug loading in the crosslinked hydrogel films was determined to be contingent upon the equilibrium swelling degree and the electrostatic interaction between MFX and the free COOH groups within the hydrogel matrix. The results pertaining to drug loading are presented in Table 4. The highest drug loading was observed in CMC HF, attributed to its high equilibrium swelling degree and substantial free COOH content. As the swellability of the hydrogel films increases, a greater volume of drug solution permeates the hydrogel matrix, resulting in the entrapment of more drug molecules within the matrix. Furthermore, the free COOH groups present in the CA crosslinked hydrogel films undergo partial ionization at aqueous pH, facilitating interaction with the amine group of MFX (pKa = 9.3).[53] This interaction can enhance the loading of MFX in CA crosslinked hydrogel films. Despite CMC HF having less swellability than HFB and HFC, it achieved the highest drug loading, probably because of its abundant free COOH content. Conversely, CMTG HF exhibited minimal drug loading, attributed to low swelling probably resulting from high crosslinking density. In the case of CA crosslinked CMC-CMTG hydrogel films, drug loading was observed to increase with the swelling of the hydrogel films, with HFA exhibiting the highest drug loading. An increase in the concentration of CMTG in the hydrogel films corresponded with a decrease in drug loading, due to reduced film swelling. This reduction may impede the diffusion of the drug into the swollen polymer matrix, resulting in a smaller quantity of drug solution being retained within the matrix. Although the TCC of these films increased from HFA to HFE, the free COOH content exerted minimal influence on the loading of MFX in these hydrogel films, with swellability having a more pronounced impact.[13,14]

***In vitro* drug release**

The *in vitro* release of MFX from the CA crosslinked hydrogel films was assessed in phosphate buffer (pH 7.4) over a 24 h period (see Fig. 8). All formulations demonstrated an initial release of approximately 15-30% of the total drug load within the first 60 min, followed by a sustained release phase. The extent of MFX released within 60 min decreased as the swellability of the hydrogel films increased. The swellability of the hydrogels depends on the degree of crosslinking. Hydrogels with greater swellability have a lower crosslinking density, meaning the hydrogel network is less tightly interconnected, allowing it to expand more when absorbing water. This increased swellability results in a larger mesh size within the hydrogel network, enabling more drug solution to be absorbed into the bulk of the hydrogel and distributed more evenly throughout the matrix rather than concentrating near the surface. This can lead to a smoother and more controlled release of the drug, as it diffuses more gradually throughout the hydrogel.[54–56] Conversely, a hydrogel with a high crosslinking density forms a tighter network with a smaller mesh size. As a result, the hydrogel exhibits restricted swelling and absorbs less drug solution. This restricted swelling forces incoming water and drug molecules to remain closer to the surface of the hydrogel. Consequently, drug concentrations can remain high at the surface, leading to a rapid release when the hydrogel is first immersed.

After 60 min, it was noted that the release of MFX from the hydrogel films was influenced by both the swellability of the films and the electrostatic interactions between MFX and the free COOH groups within the hydrogel matrix. As the swellability increased, the release of MFX appeared to slow down, likely due to the extended diffusional path length of the drug and the increased tortuosity of the swollen hydrogel films.

When hydrogel films with low crosslinking density swell, longer polymer chains exist between crosslinks. These free polymer chain units create physically entangled loop structures, reducing mesh size and potentially hindering the diffusion of the drug molecule from the hydrogel matrix.[57] Another possible reason for the controlled drug release could be the electrostatic interaction between MFX and the free COOH groups within the CA crosslinked hydrogel films at pH 7.4. At this pH, free COOH groups are typically deprotonated, existing mainly in their negatively charged carboxylate form (COO-), which can attract the positively charged MFX.[58] This interaction can slow the release of MFX from the hydrogel matrix. CMC HF exhibited faster release of MFX possibly due to the rapid rate of erosion in CMC HF. As the TCC value increased from HFA to HFE, the drug release also increased. In CMC-CMTG hydrogel films, an increase in TCC was associated with the formation of more interpolymer ester crosslinks and a decrease in free COOH groups, as more CA molecules were involved in crosslinking the polymer chains rather than remaining grafted to a single polymer chain. Consequently, the extent of electrostatic interaction between MFX and free COOH decreased as we moved from HFA to HFE.

HFE exhibited the fastest release, reaching a cumulative release of 91.10% in 6 hours. In contrast, HFA and HFB displayed more moderate profiles, releasing 69.11% and 70.26% of MFX over the same period, respectively. Despite its high swellability, HFA showed rapid drug release after 6 h, possibly due to faster erosion compared to the other CMC-CMTG hydrogel films. HFB demonstrated significant retardation ($p<0.05$) of drug release compared to CMC HF, CMTG HF, HFD, and HFE. Additionally, HFB, HFC, and HFE remained intact at the end of 24 h.

The release data were fitted into zero-order, first-order, Higuchi, and Korsmeyer-Peppas kinetic models to elucidate the drug release mechanisms from the CA crosslinked CMC-CMTG hydrogel films (see Table 5). Among all formulations, the Korsmeyer-Peppas model showed the highest correlation coefficients (R^2 = 0.995–0.999), indicating that drug release is governed by anomalous transport involving both Fickian diffusion and polymer relaxation processes. HFA and HFB achieved the most predictable release profiles, with R^2 values of 0.999 and 0.998 and n-values of 0.924 and 0.953, respectively, reflecting significant swelling-controlled release. Based on the results of good tensile strength, high swellability with less erosion, high drug loading, and better ability to control drug release compared to the other CMC-CMTG hydrogel films, HFC was identified as the optimized batch.

Hemocompatibility study

The hemolysis assay is based on the determination of the lysis of RBCs in the presence of the hydrogel films. The released haemoglobin dissolved in the external fluid, which can be measured spectrophotometrically.[31] Higher RBC damage is indicated by a high optical density value. The results of hemolysis assay of hydrogel films are given in Figure 9. All batches of crosslinked CMC-CMTG hydrogel films showed hemolysis less than 5%, indicating the hemocompatible nature of the hydrogel films. Results showed that, as the concentration of CMTG increased, the percentage of haemolysis also slightly increased.[14,31]

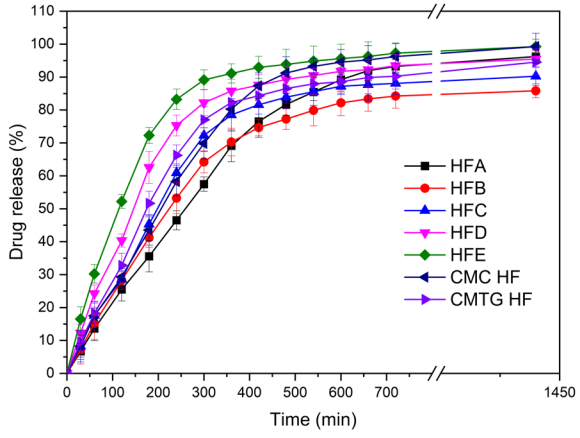

Figure 8: MFX release from hydrogel films in phosphate buffer pH 7.4

Table 5
Drug release kinetics of the hydrogel films

Batch	Zero order	First Order	Higuchi	Korsmeyer-Peppas	
	R^2	R^2	R^2	n	R^2
HFA	0.983	0.902	0.992	0.924	0.999
HFB	0.937	0.895	0.991	0.953	0.998
HFC	0.916	0.912	0.972	0.919	0.995
HFD	0.843	0.877	0.988	0.861	0.996
HFE	0.796	0.852	0.997	0.821	0.996
CMC HF	0.960	0.907	0.981	0.908	0.996
CMTG HF	0.892	0.910	0.981	0.927	0.996

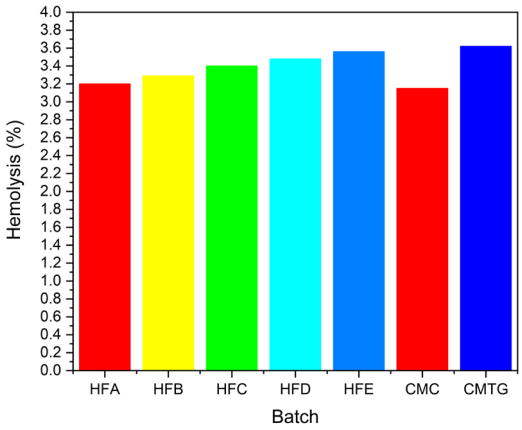

Figure 9: Hemolysis (%) of hydrogel films

The overall results indicate that the CMC-CMTG hydrogel films crosslinked with CA showed better tendency to load maximum drug and control its release while maintaining the matrix integrity, which was not found in the case of CMC and CMTG hydrogel films individually. These hydrogel films can be used as an efficient biomaterial for treatment of wounds or as implants. However, further biocompatibility and *in vivo* studies are necessary to validate their clinical applicability.

CONCLUSION

This study explored the synthesis, characterization, and application of CA crosslinked CMC-CMTG hydrogel films for controlled drug delivery. The total carboxyl content and instrumental characterization, including ATR-FTIR, TGA, and solid-state ^{13}C NMR analyses, confirmed the successful crosslinking and formation of ester linkages between CMC and CMTG. The incorporation of CMTG resulted in an increase in the contact angle and tensile strength of the hydrogel films, suggesting enhanced interpolymer crosslinking. Despite the increase in interpolymer crosslinks compared to CMC hydrogel films, the swellability of the hydrogel films with a CMC:CMTG ratio from 9:1 to 7:3 was found to be increased, possibly due to the balance of the ionic contribution of CMC and additional hydrophilic sites provided by CMTG. The drug loading in the CMC-CMTG hydrogel films was primarily dependent on the swellability of the hydrogel films. All the CMC-CMTG hydrogel films were capable of controlling drug release for up to 24 h. The release kinetics fitted well with the Korsmeyer-Peppas model, indicating non-Fickian (anomalous) diffusion as the mechanism of drug release. The overall findings support the hypothesis that combining CMC with CMTG in the presence of CA as a crosslinker could enhance the mechanical properties of the hydrogel films, without significantly affecting their swellability, thus achieving more effective control over drug release compared to hydrogel films prepared with either polymer alone.

Furthermore, hemocompatibility studies confirmed the biocompatibility of the hydrogel films, suggesting their potential for safe application in drug delivery systems involved in wound healing and implants. Future research should focus on *in vivo* evaluations and clinical applications to further validate the effectiveness of

these hydrogel films as biomaterials in medical and pharmaceutical contexts.

ACKNOWLEDGEMENTS: Authors are thankful to Adv. Vaibhav (Dada) Patil, President of Loknete Hon. Hanmantrao Patil Charitable Trust, Vita for providing necessary facilities for carrying out the research work. Shivaji University, Kolhapur and NMR facility centre of Indian Institute of Science, Bangalore, is acknowledged for assistance with analytical work. Also, authors are thankful to Apotex, Bangalore, for providing the gift sample of moxifloxacin hydrochloride.

REFERENCES

[1] E. M. Ahmed, *J. Adv. Res*., **6**, 105 (2015), https://doi.org/10.1016/j.jare.2013.07.006
[2] N. Jaramillo-Quiceno, S. Rueda-Mira, J. F. S. Marín and C. Álvarez-López, *J. Polym. Res*., **30**, 120 (2023), https://doi.org/10.1007/s10965-023-03484-1
[3] A. S. Hoffman, *Adv. Drug Deliv. Rev*., **64**, 18 (2012), https://doi.org/10.1016/j.addr.2012.09.010
[4] H. Nasution, H. Harahap, N. F. Dalimunthe, M. H. S. Ginting, M. Jaafar *et al*., *Gels*, **8**, 568 (2022), https://doi.org/10.3390/gels8090568
[5] U. G. T. M. Sampath, Y. C. Ching, C. H. Chuah, R. Singh and P.-C. Lin, *Cellulose*, **24**, 2215 (2017), https://doi.org/10.1007/s10570-017-1251-8
[6] L. O. Mota and I. F. Gimenez, *Rev. Virtual Quím*., **15**, 159 (2023), https://doi.org/10.21577/1984-6835.20220071
[7] R. J. Lewis, "Hazardous Chemicals Desk Reference", 1st ed., John Wiley & Sons, Hoboken, USA, (2008), https://doi.org/10.1002/9780470335406
[8] R. Salihu, S. I. Abd Razak, N. Ahmad Zawawi, M. R. A. Kadir, N. I. Ismail *et al*., *Eur. Polym. J*., **146**, 110271 (2021), https://doi.org/10.1016/j.eurpolymj.2021.110271
[9] V. S. Ghorpade, A. V. Yadav and R. J. Dias, *Int. J. Biol. Macromol*., **93**, 75 (2016), https://doi.org/10.1016/j.ijbiomac.2016.08.072
[10] P. L. Marani, G. D. Bloisi and D. F. S. Petri, *Cellulose*, **22**, 3907 (2015), https://doi.org/10.1007/s10570-015-0757-1
[11] P. Taylor, A. Uliniuc, U. Claude, B. Lyon, M. Polymères *et al*., *Soft Mater*., **11**, 483 (2013), https://doi.org/10.1080/1539445X.2012.710698
[12] V. S. Ghorpade, A. V. Yadav and R. J. Dias, *Carbohyd. Polym*., **164**, 339 (2017), https://doi.org/10.1016/j.carbpol.2017.02.005
[13] V. S. Ghorpade, A. V. Yadav, R. J. Dias and K. K. Mali, *J. Appl. Polym. Sci*., **135**, 46452 (2018), https://doi.org/10.1002/app.46452
[14] K. K. Mali, V. S. Ghorpade, R. J. Dias and S. C. Dhawale, *Int. J. Biol. Macromol*., **236**, 123969 (2023), https://doi.org/10.1016/j.ijbiomac.2023.123969
[15] V. S. Ghorpade, K. K. Mali, R. J. Dias, S. C. Dhawale, R. R. Digole *et al*., *Int. J. Biol. Macromol*., **282**, 137127 (2024), https://doi.org/10.1016/j.ijbiomac.2024.137127
[16] S. J. Doh, J. Y. Lee, D. Y. Lim and J. N. Im, *Fibers Polym*., **14**, 2176 (2013), https://doi.org/10.1007/s12221-013-2176-y
[17] M. Dilaver and K. Yurdakoc, *Polym. Bull*., **73**, 2661 (2016), https://doi.org/10.1007/s00289-016-1613-7
[18] K. K. Mali, S. C. Dhawale, R. J. Dias, N. S. Dhane and V. S. Ghorpade, *Indian J. Pharm. Sci*., **80**, 657 (2018), https://doi.org/10.4172/pharmaceutical-sciences.1000405
[19] A. Pettignano, A. Charlot and E. Fleury, *Polym. Rev*., **59**, 510 (2019), https://doi.org/10.1080/15583724.2019.1579226
[20] Y. Shin, D. Kim, Y. Hu, Y. Kim, I. K. Hong *et al*., *Polymers (Basel)*, **13**, 3197 (2021), https://doi.org/10.3390/polym13183197
[21] K. A. Uyanga, O. P. Okpozo, O. S. Onyekwere and W. A. Daoud, *React. Funct. Polym*., **154**, 104682 (2020), https://doi.org/10.1016/j.reactfunctpolym.2020.104682
[22] C. Demitri, R. Del Sole, F. Scalera, A. Sannino, G. Vasapollo *et al*., *J. Appl. Polym. Sci*., **110**, 2453 (2008), https://doi.org/10.1002/app.28660
[23] A. K. Nayak, D. Pal, in "Functional Biopolymers", edited by V. Thakur and M. Thakur, Springer, Cham, 2018, pp. 25, https://doi.org/10.1007/978-3-319-66417-0_2
[24] G. S. Shaw, D. Biswal, B. Anupriya, I. Banerjee, K. Pramanik *et al*., *Technol. Eng*., **56**, 141 (2017), https://doi.org/10.1080/03602559.2016.1185621
[25] K. K. Mali, S. C. Dhawale and R. J. Dias, *Int. J. Biol. Macromol*., **105**, 463 (2017), https://doi.org/10.1016/j.ijbiomac.2017.07.058
[26] A. Salam, J. J. Pawlak, R. A. Venditti and K. El-Tahlawy, *Cellulose*, **18**, 1033 (2011), https://doi.org/10.1007/s10570-011-9542-y
[27] A. M. Avachat, K. N. Gujar and K. V. Wagh, *Carbohyd. Polym*., **91**, 537 (2013), https://doi.org/10.1016/j.carbpol.2012.08.062
[28] S. Rbihi, A. Aboulouard, L. Laallam and A. Jouaiti, *Surf. Interfaces*, **21**, 100708 (2020), https://doi.org/10.1016/j.surfin.2020.100708
[29] M. M. Ahuja, *Int. J. Biol. Macromol*., **72**, 931 (2015), https://doi.org/10.1016/j.ijbiomac.2014.09.040
[30] N. H. Salunkhe, K. K. Mali, P. H. Sidwadkar, K. M. Pareek and A. S. Aundhakar, *J. Drug Deliv. Sci. Technol*., **112**, 107270 (2025), https://doi.org/10.1016/j.jddst.2025.107270
[31] B. Singh and A. Dhiman, *RSC Adv*., **5**, 44666 (2015), https://doi.org/10.1039/c5ra06857f
[32] R. Fu, C. Li, C. Yu, H. Xie, S. Shi *et al*., *Drug Deliv*., **23**, 828 (2016), https://doi.org/10.3109/10717544.2014.918676
[33] P. Costa and J. M. Sousa Lobo, *Eur. J. Pharm. Sci*., **13**, 123 (2001), https://doi.org/10.1016/S0928-0987(01)00095-1

[34] R. K. Singh and O. P. Khatri, *J. Microsc*., **246**, 43 (2012), https://doi.org/10.1111/j.1365-2818.2011.03583.x
[35] G. Priya, U. Narendrakumar and I. Manjubala, *J. Therm. Anal. Calorim*., **138**, 89 (2019), https://doi.org/10.1007/s10973-019-08171-2
[36] T. V. C. McOscar and W. M. Gramlich, *Cellulose*, **25**, 6531 (2018), https://doi.org/10.1007/s10570-018-2015-9
[37] S. H. Aswathy, U. NarendraKumar and I. Manjubala, *Polymers (Basel)*, **14**, 4669 (2022), https://doi.org/10.3390/polym14214669
[38] G. Kaur, M. Mahajan and P. Bassi, *Int. J. Polym. Mater*., **62**, 475 (2013), https://doi.org/10.1080/00914037.2012.734348
[39] L. Yan, X. Dang, M. Yang, W. Han and Y. Li, *ACS Sustain. Chem. Eng*., **11**, 7323 (2023), https://doi.org/10.1021/acssuschemeng.2c07302
[40] N. Pahimanolis, A. Salminen, P. A. Penttilä, J. T. Korhonen, L.-S. Johansson *et al*., *Cellulose*, **20**, 1459 (2013), https://doi.org/10.1007/s10570-013-9923-5
[41] S. Bandyopadhyay, N. Saha, U. V. Brodnjak and P. Sáha, *Food Packag. Shelf Life*, **22**, 100402 (2019), https://doi.org/10.1016/j.fpsl.2019.100402
[42] S. Dong, S. Feng, F. Liu, R. Li, W. Li *et al*., *Int. J. Biol. Macromol*., **179**, 398 (2021), https://doi.org/10.1016/j.ijbiomac.2021.03.027
[43] M. A. P. Morais, M. Silva, M. Barros, P. Halley, Y. Almeida *et al*., *J. Appl. Polym. Sci*., **141**, 44 (2024). https://doi.org/10.1002/app.56162
[44] G. F. Levchik, K. Si, S. V. Levchik, G. Camino and C. A. Wilkie, *Polym. Degrad. Stab*., **65**, 395 (1999), https://doi.org/10.1016/S0141-3910(99)00028-2
[45] T. Takács, M. M. Abdelghafour, D. Sebők, Á. Kukovecz and L. Janovák, *J. Therm. Anal. Calorim*., **149**, 2765 (2024), https://doi.org/10.1007/s10973-023-12862-2
[46] S. L. Madorsky and S. Straus, *J. Res. Natl. Bur. Stand. Sect. A Phys. Chem*., **63A**, 261 (1959), https://doi.org/10.6028/jres.063A.020
[47] V. S. Ghorpade, R. J. Dias, K. K. Mali and S. I. Mulla, *J. Drug Deliv. Sci. Technol*., **52**, 421 (2019), https://doi.org/10.1016/j.jddst.2019.05.013
[48] K. M. N. Silva, D. É. L. de Carvalho, V. M. M. Valente, J. C. Campos Rubio, P. E. Faria *et al.*, *Int. J. Biol. Macromol*., **126**, 359 (2019), https://doi.org/10.1016/j.ijbiomac.2018.12.136
[49] I. Ayouch, I. Kassem, Z. Kassab, I. Barrak, A. Barhoun *et al.*, *Surf. Interfaces*, **24**, 101124 (2021), https://doi.org/10.1016/j.surfin.2021.101124
[50] H. Chopra, I. Singh, S. Kumar, T. Bhattacharya, M. H. Rahman *et al.*, *Curr. Drug Deliv*., **19**, 658 (2022), https://doi.org/10.2174/1567201818666210601155558
[51] X. Feng and R. Pelton, *Macromolecules*, **40**, 1624 (2007), https://doi.org/10.1021/ma062608j
[52] K. Pratinthong, W. Punyodom, P. Jantrawut, K. Jantanasakulwong, W. Tongdeesoontorn *et al*., *Polymers (Basel)*, **16**, 1798 (2024), https://doi.org/10.3390/polym16131798
[53] A. Sharapova, M. Ol'khovich, S. Blokhina, E. Zhirova and G. Perlovich, *J. Mol. Liq*., **339**, 116814 (2021), https://doi.org/10.1016/j.molliq.2021.116814
[54] G. Thakur, A. Mitra, D. Rousseau, A. Basak, S. Sarkar *et al*., *J. Mater. Sci. Mater. Med*., **22**, 115 (2011), https://doi.org/10.1007/s10856-010-4185-3
[55] J. Long, A. V. Nand, C. Bunt and A. Seyfoddin, *Pharm. Dev. Technol*., **24**, 839 (2019), https://doi.org/10.1080/10837450.2019.1602632
[56] S. L. Jahren, M. F. Butler, S. Adams and R. E. Cameron, *Macromol. Chem. Phys*., **211**, 644 (2010), https://doi.org/10.1002/macp.200900560
[57] F. V. Lavrentev, V. V. Shilovskikh, V. S. Alabusheva, V. Y. Yurova, A. A. Nikitina *et al*., *Molecules*, **28**, 5931 (2023), https://doi.org/10.3390/molecules28155931
[58] H. A. Al-Abadleh, A. L. Mifflin, P. A. Bertin, S. T. Nguyen and F. M. Geiger, *J. Phys. Chem. B*, **109**, 9691 (2005), https://doi.org/10.1021/jp050782o